

Improving the Convergence of the Iterative Implicit Monte Carlo Method of Thermal Radiation Transport

N. A. Gentile*, Simon Bolding†, and Ben C. Yee‡

*Lawrence Livermore National Laboratory, L-38
7000 East Avenue
Livermore, CA 94551

†Department of Nuclear Engineering
Texas A&M University
College Station, TX 77843-3133

‡Department of Nuclear Engineering & Radiological Sciences
University of Michigan, Ann Arbor, Michigan 48109

* gentile1@llnl.gov

Abstract Thermal radiation transport simulations are sensitive to the value of T used in the thermal emission source term. Monte Carlo thermal radiation transport simulations typically employ the Fleck and Cummings [1] semi-implicit approximation or emission temperature, which uses the t_n value of temperature. This can lead to thermodynamically incorrect behavior, such as matter temperatures which exceed the temperature of adjacent radiation sources [2]. This work describes work on a Monte Carlo thermal radiation transport algorithm which is fully implicit in the emission temperature. This algorithm calculates the value of T_{n+1} for use in the thermal emission term in an iterative way.

I. INTRODUCTION

A Monte Carlo thermal radiation transport method that is fully implicit in the value of matter temperature used to calculate thermal emission was described in [3] and [4]. This method involves generating a sequence of underestimates of the matter temperature T in each zone until convergence at the end of time-step value of T is obtained. These underestimates were produced by ignoring the reabsorption of thermally emitted photons. Thus the method is considerably more expensive than IMC for simulations with cold opaque regions, where thermal emission and reabsorption are large. The current work describes a modification of the method that allows the inclusion of an approximation of the amount of reabsorption. This increases the values of T in the sequence of estimates, and reduces the number of iterations required. We demonstrate accurate solutions of two test problems, and demonstrate a reduction in the number of iterations required compared to the original method.

II. THEORY

The time-dependent frequency-independent transport equation for photons is [5]

$$\begin{aligned} \frac{1}{c} \frac{\partial I}{\partial t} + \Omega \cdot \nabla I &= -\sigma_t I + \frac{1}{4\pi} c \sigma_a(T) a T^4 \\ &+ \int_{4\pi} d\Omega' \sigma_s I \\ &+ S, \end{aligned} \quad (1)$$

where $I(x, t, \Omega)$ is the radiation intensity, with units of energy/(time length² solid angle), T is the material temperature, $\sigma_a(T)$ is the macroscopic absorption opacity in inverse length units, $\sigma_s(T)$ is the macroscopic scattering opacity in inverse length units, and $\sigma_t = \sigma_a + \sigma_s$, and $S(x, t, \Omega)$ is a time

and space-dependent radiation source; c is the speed of light, and $a = \frac{8\pi^5 k^4}{15c^3 h^3}$ is the radiation constant. Eq.(1) comes with initial conditions $I_{ic}(x, t, \Omega)$ defined for all points in the region of interest, and boundary conditions $I_{bc}(x, t, \Omega)$ defined on the boundary of the region of interest for values of Ω that ensure that I_{bc} describes incoming photons.

The transport equation is coupled to the material energy balance equation [5]

$$\frac{\partial e_m}{\partial t} = \rho c_v \frac{\partial T}{\partial t} = \int_{4\pi} \sigma_a I d\Omega - c \sigma_a a T^4. \quad (2)$$

Here, $e_m(\rho, T)$ is the equation of state, which gives the matter energy density in units of energy/length³ as a function of the mass density and temperature, ρ is the mass density in units of mass/length³, and c_v is the heat capacity in units of energy/(mass – temperature). Thermodynamics requires that $\partial e_m / \partial T \geq 0$; otherwise, the material could reach a lower energy state by becoming warmer. Eq.(2) is simply a statement of energy conservation; it states that the change in energy of the material is equal to the negative of the change in the energy of the radiation field represented by I . In this paper, we will assume that ρ is constant in time.

Eqs. (1) and (2) are often solved by Monte Carlo methods. These methods advance solutions of Eqs. (1) and (2) over a time interval $[t_n, t_n + \Delta t]$ that is small enough that we can regard σ_a and σ_s as fixed at their t_n values. Even for small values of Δt , however, it is not possible to use $T_n \equiv T(t_n)$ in the thermal emission terms in Eqs.(1) and (2) without encountering instabilities; eliminating these instabilities is the reason for the development of the Implicit Monte Carlo (IMC) algorithm [1]. IMC uses a semi-implicit approximation to get an estimate of the matter temperature at $t_n + \Delta t$. The effect of this approximation is to modify Eqs. (1) and (2) by multiplying the absorption opacity by a factor

$$f_a = \frac{1}{1 + \beta c \Delta t \sigma_a}, \quad (3)$$

where $f_a \in (0, 1)$, and adding an equal amount of thermally redistributed isotropic scattering. (Here $\beta \equiv \frac{4aT^3}{\rho c_v}$.) This “effective scattering” approximately models absorption and re-emission. Although the instabilities are eliminated by IMC [6], thermodynamically inconsistent matter and radiation temperatures can still result in simulations with large values of Δt . That is, the simulation may produce zones with temperatures higher than that of a Planckian source illuminating the zones. It has been rigorously shown that the actual solutions of Eqs. (1) and (2) do not violate this “maximum principle” [7] [8] [9] [10] [2]. The maximum principle states that if the initial and boundary conditions for a problem lie between two Planck functions, then the specific intensity will always lie between the two Planck functions for all points inside the system and all times after the initial time [11].

A common situation in which IMC simulations violate the maximum principle is when a zone with a large temperature is adjacent to one that is at much lower temperature. Unless the time step is very small [2], a large amount of thermally emitted radiation will flow from the hot zone into the cold zone. The energy absorbed from this radiation will heat the cold zone. But the thermal emission of the initially cold zone is calculated using the initial, small temperature. This means that the initially cold zone cannot re-radiate the energy it is absorbing from the hot zone in the current time step. The large amount of absorption coupled with the small, incorrect, amount of emission can lead to the initially cold zone becoming hotter than the initially hot zone in the next time step, in clear violation of the laws of thermodynamics. This scenario illustrates the fact that the lack of implicit time differencing of the thermal emission - that is, the failure to use T_{n+1} to calculate the amount of thermal emission - leads to violations of the maximum principle [7].

Besides violations of the maximum principle, another drawback of the IMC method is long run times in problems with large opaque regions. This is caused by the effective scattering. Large values of σ_a can make f_a nearly zero. This replaces almost all of the absorption by effective scattering. The particles in the IMC simulation execute many relatively expensive scatters in opaque regions, leading to long run times.

As described in [3] and [4], the Iterative Implicit Monte Carlo (IIMC) method was developed to prevent violations the maximum principle. This method does not introduce effective scattering. Instead, it iterates on the temperature used to calculate thermal emission. The effective scattering is replaced by multiple iterations during each time step, during which new thermal source particles are produced at a sequence of increasing temperatures. The cost of effective scattering, which increases the number of segments taken by each Monte Carlo particle, is replaced by the need to perform a one-dimensional non-linear root find in each zone during each iteration.

The result of the iteration in IIMC is to produce a numerical solution of Eqs.(1) and (2) in which the temperature used in the thermal emission term term is the t_{n+1} value. Although the opacity used in this numerical solution of remains the t_n value, the use of T_{n+1} for calculating the magnitude of thermal emission is frequently sufficient to ensure that the solution will satisfy the maximum principle [11].

IIMC is derived as follows. We take advantage of the

linearity of Eq. (1) in I to separate it into 3 parts, only one of which contains the non-linear term in T . We represent I as the sum of three quantities, $I_c + I_s + I_t$. These quantities model the photons that result from the initial conditions, radiation sources and boundary conditions, and thermal emission respectively. In what follows, we will assume that we can use t_n values of the opacity, but we will construct an estimate of the t_{n+1} value of the temperature for thermal emission.

First, we will model the effects of the initial conditions. We will chose I_c to satisfy the equation

$$\frac{1}{c} \frac{\partial I_c}{\partial t} + \Omega \cdot \nabla I_c = -\sigma_t(T_n)I_c + \int_{4\pi} d\Omega' \sigma_s(T_n)I_c, \quad (4)$$

with the initial condition $I_c(t_n) = I_{ic}$ and boundary condition $I_c = 0$ on the boundary of the region of interest. Note that, because we have fixed the opacities at their value at t_n , this equation is independent of T . (Henceforth, we will not explicitly show the temperature dependence of the opacities, since all will be evaluated at the beginning of time step temperature T_n .) In the first time step, I_{ic} describes the initial conditions of the problem. In subsequent time steps, it describes the value of I at the end of the previous time step. In a Monte Carlo simulation, I_{ic} would be represented by the census particles; that is, particles which have reached t_n in the previous time step without being absorbed or leaving the problem.

Next, we will model the effects of any radiation sources. We will chose I_s to satisfy the equation

$$\frac{1}{c} \frac{\partial I_s}{\partial t} + \Omega \cdot \nabla I_s = -\sigma_t I_s + \int_{4\pi} d\Omega' \sigma_s I_s + S \quad (5)$$

with initial condition $I_s(t_n) = 0$ and boundary condition $I_s = I_{bc}$ on the boundary of the region of interest. Note that this equation, like Eq. (4), is independent of T .

We determine the equation satisfied by I_t by inserting $I_c + I_s + I_t$ into Eq. (1) and subtracting Eqs. (4) and (5) from it, and using $T_{n+1} \equiv T(t_{n+1})$ in the thermal emission term. The result is

$$\frac{1}{c} \frac{\partial I_t}{\partial t} + \Omega \cdot \nabla I_t = -\sigma_t I_t + c\sigma_a a [T_{n+1}]^4 + \int_{4\pi} d\Omega' \sigma_s I_t, \quad (6)$$

with initial condition $I_t(t_n) = 0$ and boundary condition $I_t = 0$ on the boundary of the region of interest. This equation models the effects of thermally emitted photons. Unlike Eqs. (4) and (5), this equation contains the non-linear term in T . Written in terms of $I_c, I_s,$ and I_t , Eq. (2) becomes

$$\frac{\partial e_m}{\partial t} = \int_{4\pi} \sigma_a [I_c + I_s + I_t] d\Omega - c\sigma_a a [T_{n+1}]^4. \quad (7)$$

In a numerical simulation, we will integrate this equation over the time step and solve the resulting equation, which is

$$\frac{e_m(T_{n+1}) - e_m(T_n)}{\Delta t} = \int_{t_n}^{t_{n+1}} \int_{4\pi} \sigma_a [I_c + I_s + I_t] d\Omega dt - c\sigma_a a [T_{n+1}]^4. \quad (8)$$

Here, $\Delta t \equiv t_{n+1} - t_n$. Eq.(8) is a statement of energy conservation over the time step.

Solving Eqs. (4) and (5) by Monte Carlo is straightforward because they do not depend on the unknown value T_{n+1} . This

leaves only the problem of solving Eq. (6) for $I_t(t)$ and Eq. (8) for $T(t_{n+1})$.

For notational convenience, we are going to define the transport operator $\mathcal{T}(I)$:

$$\mathcal{T}(I) \equiv \frac{1}{c} \frac{\partial I}{\partial t} + \Omega \cdot \nabla I + \sigma_t I - \int_{4\pi} d\Omega' \sigma_s I. \quad (9)$$

We express I_t as a series:

$$I_t = I_t^0 + I_t^1 + \dots + I_t^i + \dots = \sum_{i=0}^{\infty} I_t^i. \quad (10)$$

(Here i is an index; it does not indicate raising I_t to a power. We are using a superscript for this iteration index to avoid confusion with the subscripts that we are using to indicate time centering.) Substituting Eq.(10) into Eq.(6) yields

$$\mathcal{T} \left(\sum_{i=0}^{\infty} I_t^i \right) = \sum_{i=0}^{\infty} \mathcal{T}(I_t^i) = \frac{1}{4\pi} c\sigma_a a [T_{n+1}]^4. \quad (11)$$

The equation satisfied by T_{n+1} is determined by substituting Eq.(10) into Eq.(8), yielding

$$\begin{aligned} e_m(T_{n+1}) - e_m(T_n) &= \int_{t_n}^{t_{n+1}} \int_{4\pi} \sigma_a (I_c + I_s) d\Omega dt \\ &+ \sum_{i=0}^{\infty} \int_{t_n}^{t_{n+1}} \int_{4\pi} \sigma_a I_t^i d\Omega dt \\ &- c\sigma_a a [T_{n+1}]^4 \Delta t. \end{aligned} \quad (12)$$

We also represent the temperature source with a sequence of values T^i , which satisfy

$$\begin{aligned} \mathcal{T}(I_t^0) &= \frac{1}{4\pi} c\sigma_a a [T^0]^4, \\ \mathcal{T}(I_t^1) &= \frac{1}{4\pi} c\sigma_a a [(T^1)^4 - (T^0)^4], \\ &\dots \\ \mathcal{T}(I_t^i) &= \frac{1}{4\pi} c\sigma_a a [(T^i)^4 - (T^{i-1})^4], \end{aligned} \quad (13)$$

where we have not defined the T^i yet. As T^{i-1} approaches T^i , the magnitude of the thermal source term is reduced. If the sequence of expressions in Eq. (13) are summed over i , the source terms cancel in pairs and leave us with

$$\mathcal{T} \left(\sum_{i=0}^{\infty} I_t^i \right) = \sum_{i=0}^{\infty} \mathcal{T}(I_t^i) = \frac{1}{4\pi} c\sigma_a a (T^\infty)^4, \quad (14)$$

where T^∞ is the value to which the sequence of T^i converges (assuming that the sequence does converge).

In [3] and [4], the T^i were chosen to satisfy the following non-linear equation:

$$\begin{aligned} e_m(T^i) - e_m(T_n) &= \int_{t_n}^{t_n + \Delta t} \int_{4\pi} \sigma_a \left[I_c + I_s + \sum_{j=0}^{i-1} I_t^j \right] d\Omega dt \\ &- c\sigma_a a (T^i)^4 \Delta t. \end{aligned} \quad (15)$$

This equation defines $e_m(T^i)$ to be $e_m(T_n)$ added to the amount of energy absorbed from the photons representing I_c and I_s and the amount of energy absorbed from the photons representing I_t^0 through I_t^{i-1} , minus the amount emitted at the temperature T^i . That is, we are defining T^i to be the temperature that would result if a) the absorption from all initial and source photons is accounted for, b) the emission and absorption from all previous iterations of thermally emitted photons is accounted for, and c) the emission but not the absorption of photons from the current iteration are accounted for. The last point is crucial, because it ensures that $T^i \leq T^{i+1}$; see [3] for a proof. This is a desirable property, because it ensures that the source terms in Eq. (13) will be positive, ensuring that their Monte Carlo representation will be particles with positive energy.

While using Eq. (15) to calculate the sequence of T^i produced results which did not violate the maximum principle on a variety of problems, the sequence of T^i converged slowly in problems with large opacities. This occurred because Eq. (15) includes the effects of emission but ignores the reabsorption of thermally emitted photons, thus underestimating T_{n+1} . When the amount of emission and reabsorption is large, ignoring the latter makes T^i a large underestimate of T_{n+1} .

In order to speed up the convergence, we choose to approximate, rather than ignore, the reabsorption of thermally emitted photons in the zone. We replace Eq. (15) with

$$\begin{aligned} e_m(T^i) - e_m(T_n) &= \int_{t_n}^{t_n + \Delta t} \int_{4\pi} \sigma_a \left[I_c + I_s + \sum_{j=0}^{i-1} I_t^j \right] d\Omega dt \\ &- c\sigma_a a [T^{i-1}]^4 \Delta t \\ &- (1 - f_R^i) c\sigma_a a [T^i]^4 - a [T^{i-1}]^4 \Delta t, \end{aligned} \quad (16)$$

where f_R^i is an estimate of the fraction of thermally emitted photons for iteration i that are reabsorbed. In Eq.(16), the second line on the right-hand side represents the total thermal emission from iterations $0 - i - 1$, i.e., the sum of the source terms for those iterations in Eq.(13). The third line represents the thermal emission source for iteration i , with the fraction which is reabsorbed subtracted off.

In order to obtain f_R^i , the estimate of reemission, we modify the Monte Carlo solution technique for I_t . After solving for $I_c + I_s$, we emit simulation particles, representing thermal photons, that have an unknown weight. Nominally, they are assigned a weight of $\frac{1}{N_z}$, where N_z is the number of these simulation particles in the zone. These simulation particles are tracked until they reach either census (that is, reach n^{n+1}) or the boundary of the zone in which they were emitted. Their energy is decreased along each segment of length l_s via absorption to $\frac{1}{N_z} \exp[-\sigma_a l]$. When all of these simulation particles reach either census or the zone boundary, we estimate f_R^i in each zone via a sum over all segments executed by each simulation particle in the zone :

$$f_R^i = \frac{1}{N_z} \sum_{photons} (1 - \exp[-\sigma_a \sum_s l_s]). \quad (17)$$

As calculated by Eq.(17), $f_R^i \in [0, 1]$. This value of f_R^i is used in Eq. (16) to obtain the next value of T^i . With T^i calculated, the source term in Eq. (13) is then known. This let us assign

physical energies to each simulation particle in every zone. After this is done, we advance the simulation particles the rest of the way through the time step, that is, until each one reaches census, is completely absorbed, or leaves the problem through a boundary. This completes the calculation of I_i^i . The process is repeated for the next iteration, with each iteration i using a new value of f_R^i , until each zone satisfies

$$\frac{c\sigma_a[(T^i)^4 - (T^{i-1})^4]dt}{\rho c_v T^i} < 10^{-8}, \quad (18)$$

i.e., until the source term for thermal emission in Eq.(13) in each zone is small compared to the thermal energy in that zone. At that point, the iteration is terminated. Note that the iteration continues in every zone until all zones satisfy Eq.18).

We desire that the values of T^i obtained from using Eq.(16) in place of Eq.(15) still satisfy $T^i \leq T^{i+1}$, so as to prevent the occurrence of a negative source in Eq.(13). Using Eq(16), we find that

$$\begin{aligned} e_m(T^{i+1}) - e_m(T^i) &= \left[\int_{t_n}^{t_n+\Delta t} \int_{4\pi} \sigma_a I_t^i d\Omega dt \right. \\ &- \left. f_R^i c\sigma_a(a[T^{i-1}]^4 - a[T^i]^4)\Delta t \right] \\ &- (1 - f_R^{i+1})c\sigma_a(a[T^{i+1}]^4 - a[T^i]^4)\Delta t. \end{aligned} \quad (19)$$

First, consider the term in brackets. The term $f_R^i c\sigma_a(a[T^{i-1}]^4 - a[T^i]^4)$ is the fraction of the energy emitted in iteration i which is reabsorbed in the zone in which it was emitted. The integral $\int_{t_n}^{t_n+\Delta t} \int_{4\pi} \sigma_a I_t^i d\Omega dt$ is the amount of thermal energy emitted anywhere in iteration i which was absorbed in the zone. Thus, the term on the right-hand side in brackets is positive. Next, consider the term $e_m(T^{i+1}) - e_m(T^i)$. Since, as mentioned previously, thermodynamics requires that $\partial e_m / \partial T \geq 0$, the sign of $e_m(T^{i+1}) - e_m(T^i)$ must be the same as the sign of $T^{i+1} - T^i$, and thus of $[T^{i+1}]^4 - [T^i]^4$. Since Eq.(19) requires that the sum of $e_m(T^{i+1}) - e_m(T^i)$ and $(1 - f_R^{i+1})c\sigma_a(a[T^{i+1}]^4 - a[T^i]^4)\Delta t$ equals the positive term in brackets, both terms must be positive, which ensures that $T^i \leq T^{i+1}$.

For convenience, in this work we will refer to the Iterative Implicit Monte Carlo method using Eq. (16) to calculate the T^i as Reabsorption IIMC (RIIMC), while the original method, using Eq. (15), will be referred to as IIMC.

III. RESULTS AND ANALYSIS

We will apply RIIMC and IIMC to two test problems. One test has non-opaque zones and one has opaque zones. We will compare the number of iterations required to reach convergence. We will also compare the answers to the results of IMC simulations.

We will first apply the methods to the Su-Olson volume source test problem [12]. In this benchmark, $a = c = 1$, $\rho = 1$, $c_v = 4 T_m^3$, and $\sigma_a = \sigma_s = 0.5$. At $x = 0$ there is a reflecting boundary and at large x there is a vacuum boundary. A volume radiation source with an emission rate of 1 per unit volume per unit time is located between $x = 0$ and $x = 0.5$, and is turned on between $t = 0$ and $t = 10$. The mesh has 200 zones which span $x \in [0, 5]$. Since $\sigma_a \Delta x = 1.25 \times 10^{-2}$,

we expect that only a small amount of the thermally emitted energy will be reabsorbed in the zone from which it is emitted. Results were obtained at $t = 10$ with $\Delta t = 0.1$. The IMC simulation used 10^5 particles per cycle; the IIMC and RIIMC simulations used 10^5 particles per iteration.

Figure 1 shows that the computed material and radiation energy densities for all three methods agree with the analytic solution. Both RIIMC and IIMC average 8 iterations per time step. For this problem, the amount of thermal energy reabsorbed in the zone in which it is emitted, calculated by Eq.(17), is approximately 1.22×10^{-2} . With this small value, the use of Eq. (16) in place Eq. (15) does not reduce the number of iterations.

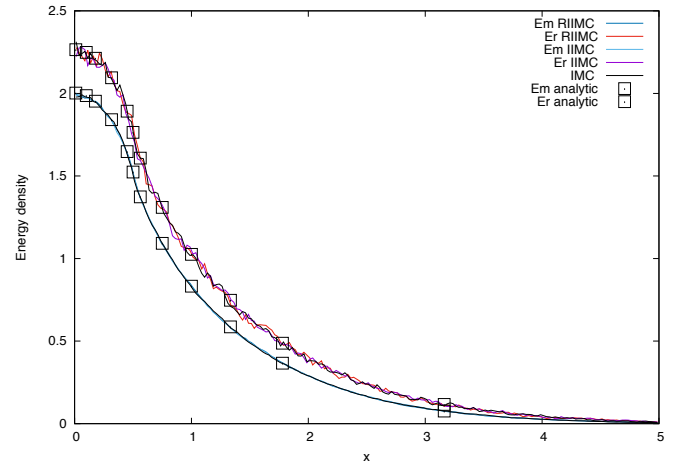


Fig. 1. Material and radiative energy densities vs. position at time 10 for the Su-Olson problem using RIIMC, IIMC, and IMC. The reference solution from [12] is also indicated on the plots.

The second test is a Marshak wave in a medium with a temperature-dependent opacity, described in [13]. In this benchmark, $\sigma_a = \frac{10 \text{keV}^3 \text{cm}^{-1}}{T^3}$, $\sigma_s = 0$, $\rho = 3.0 \frac{\text{g}}{\text{cm}^3}$ and $c_v = 10^{15} \frac{\text{erg}}{\text{g-keV}}$. The initial temperature is $T_0 = 0.1$ keV. At $x = 0$ there is a constant temperature source at 1 keV and at large x there is a vacuum boundary. The mesh has 100 zones which span $x \in [0, 0.1]$. Since $\sigma_a(T_0) \Delta x = 10$, we expect that a large fraction of the thermally emitted energy will be reabsorbed in the zone from which it is emitted. Results were obtained at $t = 10^{-10}$ s with both $\Delta t = 10^{-11}$ s and $\Delta t = 10^{-12}$ s. The IMC simulation used 10^5 particles per cycle; the IIMC and RIIMC simulations used 10^5 particles per iteration.

Figure 2 shows that the computed material temperature for all three methods at $t = 10^{-10}$ s with both values of Δt .

Using the smaller value of Δt , IMC, IIMC, and RIIMC produce similar results. None of the three methods shows a violation of the maximum principle - the matter temperature in all zones is less than the temperature of the face source, 1 keV. With the larger value of Δt , the results of IMC and the iterative methods are different. IMC violates the maximum

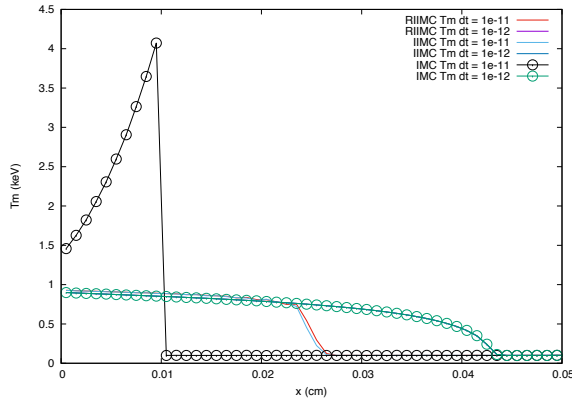


Fig. 2. Material temperature vs. position at time 10^{-10} s from RIIMC, IIMC, and IMC. Simulations using both $\Delta t = 10^{-11}$ s and $\Delta t = 10^{-12}$ s are shown.

principle, reaching a temperature exceeding 4 keV near the wave front. By contrast, in the solutions generated by the iterative methods, all zones have temperatures less than the source temperature of 1 keV.

Although they do not violate the maximum principle, the results of the IIMC and RIIMC with large Δt do not agree well with the results with small Δt . The wave front does not advance as far when Δt is large. This happens because the opacity is a strong function of temperature, and the large time step cannot resolve the rapid change in the opacity with time as the material is heated by the source. While IIMC and RIIMC cannot produce accurate results with a large time step, they produce thermodynamically consistent results, while IMC does not.

With $\Delta t = 10^{-12}$ s, IIMC averages 10 iterations per time step, while RIIMC averages 6. With this value of Δt , the fraction of thermal energy reabsorbed in the zone in which it is emitted is approximately 0.75. The use of Eq. (16) in place Eq. (15) moderately reduces the number of iterations.

With $\Delta t = 10^{-11}$ s, IIMC averages 390 iterations per time step, while RIIMC averages 34. With this value of Δt , the fraction of thermal energy reabsorbed in the zone in which it is emitted is approximately 0.85. The use of Eq. (16) in place Eq. (15) significantly reduces the number of iterations for this case.

The reduction in the number of iterations for the large Δt case shows up in the run time. Running on a single 2.8 GHz Intel Core i7, the IMC simulation took 3.2 minutes, while the RIIMC took 20 seconds. This is still not competitive with the (thermodynamically inconsistent) IMC simulation, which took under 2 seconds.

Run times for the iterative methods for the small Δt case, which requires fewer iterations, are closer to the IMC run time. IMC takes 21.8 seconds in that case; IIMC takes 56.8 seconds, while RIIMC takes 42.6 seconds.

Figure 3 shows the matter temperature as a function of space for all of the iterations that take place in the first time step of a simulation of the Marshak test problem. The simu-

lation used the larger time step value, with $\Delta t = 10^{-11}$ s. The region shown has $x \in [0, 0.006 \text{ cm}]$, which contains the first six zones of the simulation. These are the zones for which the temperature changes appreciably during the first time step.

This plot illustrates the way that T^i changes with increasing i and increasing distance from the temperature source located at $x = 0$. On the first iteration, the first zone, closest to the source, reaches a large temperature, while the other zones remain cold. On the next iteration, the second zone increases in temperature, while the temperature of the first zone changes very little. On the third iteration, the third zone increases in temperature. This happens because of the large opacity of the problem at the initial temperature. Radiation from the face source can only penetrate into the first zone, so only that zone increases in temperature in the first iteration. On the second iteration, radiation from the first zone, which was heated on the first iteration, heats the second zone. On the third iteration, the second zone can heat the third zone, and also the first zone. This process continues in later iterations until the coupling between the face source and the zones heated by it is simulated. This process suggests that the number of iterations required by the RIIMC method must be larger than the number of zones contained in the distance through which the Marshak wave travels in a time step. It also suggests that the number of iterations could be lowered if a way was found to couple the zones together more implicitly.

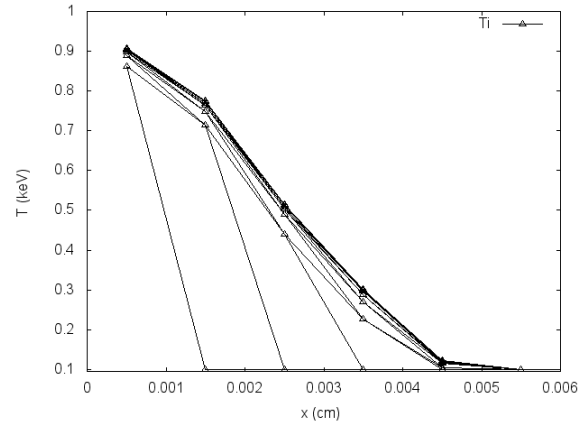


Fig. 3. Matter temperature for all iterations vs. position for the first six zones during the first time step (with $\Delta t = 10^{-11}$ s) of the Marshak test problem using RIIMC.

IV. CONCLUSIONS

A modification of the Iterative Implicit Monte Carlo method which demonstrates improved convergence for problems with opaque materials is presented. The modification preserves the property which motivated the development of IIMC, which is that it is fully implicit in the matter temperature, and thus does not violate the maximum principle. Although this modification substantially decreases the amount of work done during the simulation for problems with a large opacity, further improvements are needed to make it competitive in run time with the IMC method.

V. ACKNOWLEDGMENTS

This work performed under the auspices of the U.S. Department of Energy by Lawrence Livermore National Security, L.L.C. under Contract De-AC52-07NA27344.

REFERENCES

1. J. A. Fleck, Jr., and J. D. Cummings, "An Implicit Monte Carlo Scheme for Calculating Time and Frequency Dependent Nonlinear Radiation Transport," *J. Comput. Phys.*, **8**, pp. 313-342 (1971).
2. E. W. Larsen and B. Mercier, "Analysis of a Monte Carlo method for nonlinear radiative transfer" *J. Comput. Phys.* **71**, pp.50-64 (1987).
3. N. A. Gentile and B. C. Yee, "Iterative Implicit Monte Carlo" *J. Comput Theor. Transport*, **45**, pp. 71-98 (2016).
4. B. C. Yee and N. A. Gentile, "Iterative Implicit Monte Carlo" *Trans. Am. Nucl. Soc.*, **111**, pp. 641-644 (2014).
5. G. C. Pomraning, "Equations of Radiation Hydrodynamics", in International Series of Monographs in Natural Philosophy, edited by D. ter Harr (Pergamon, New York, 1973), Vol. 54.
6. A. B. Wollaber, "Four Decades of Implicit Monte Carlo," *J. Comput Theor. Transport*, **45**, pp. 1-70 (2016).
7. E.S. Andreev, M.Yu. Kuzmanov, E.B. Rachilov, *U.S.S.R. Comput. Math. Math. Phys.* **23** p. 104 (1983).
8. B. Mercier, "Application of accretive operators theory to radiative transfer equations", *SIAM J. Math. Anal.* **18** p. 393 (1987).
9. J.D. Densmore, E.W. Larsen, "Asymptotic equilibrium diffusion analysis of time-dependent Monte Carlo methods for Grey radiative transfer", *J. Comput. Phys.* **199** p. 175 (2004).
10. D.A. Knoll, R.B. Lowrie, J.E. Morel, "Numerical analysis of time integration errors for nonequilibrium radiation diffusion", *J. Comput. Phys.* **226** p. 1332 (2007).
11. E. W. Larsen, A. Kumar, and J. E. Morel, "Properties of the Implicitly Time-differenced Equations of Thermal Radiation Transport" *J. Comput. Phys.*, **238**, pp. 82-96 (2013).
12. Bingjing Su and Gordon L. Olson, "An Analytical Benchmark for Non-equilibrium Radiative Transfer in an Isotropically Scattering Medium," *Ann. Nucl. Energy* **24**, pp. 1035-1055 (1997).
13. M. A. Cleveland and A. B. Wollaber, "Corrected Implicit Monte Carlo", in preparation.